Progress In Electromagnetics Research M, Vol. 107, 35–49, 2022

Design of Penta-Band Notched UWB MIMO Antenna for Diverse Wireless Applications

Ramesh B. Sadineni[1, *] and Dinesha P. Gowda[2]

Abstract—In this manuscript, the realization of penta-band notches with the aid of an ultra-wideband (UWB) multiple-input multiple-output (MIMO) antenna for diverse wireless applications is demonstrated. A single port UWB antenna is utilized to construct the proposed MIMO antenna, which comprises an altered patch loaded with three U-shape slots and an inverse U-shape slot on the feed line followed by a C-shape stub adjacent to the feed line. These slots and C-shape stub are liable to generate five notches at 3.4 GHz (3.16–3.67 GHz), 4 GHz (3.88–4.10 GHz), 4.6 GHz (4.56–4.75 GHz), 5.7 GHz (5.65–5.92 GHz), and 7.8 GHz (7.39–8.12 GHz), respectively. These notches depreciate interference from WiMAX, lower C-band, WLAN, and X-band (satellite communication) frequencies. Alternatively, the reported antenna can also be utilized as a proximity radar (8–12 GHz) in X-band. The proposed antenna engraved on a Rogers RT/Duroid 5880 substrate having an overall size of $80 \times 80 \times 1.6\,\text{mm}^3$ or $0.8\lambda_0 \times 0.8\lambda_0 \times 0.016\lambda_0$ (λ_0 is the free-space wavelength at lowest frequency 3 GHz). Simulation and experimentation have been performed to corroborate the performance of the reported antenna. Results emphasize that the proposed MIMO antenna operates from 3 GHz to 14 GHz with measured peak gain 4.8 dBi, radiation efficiency above 83%, and isolation less than −20 dB. Except at notches, the computed envelope correlation coefficient (ECC) is less than 0.03; diversity gain (DG) is approximately 10; total active reflection coefficient (TARC) is less than −10 dB; channel capacity loss (CCL) less than 0.35 bps/Hz. These characteristics qualify it as a multifunctional antenna for wireless applications, lowering the antenna count needed in compact wireless devices.

1. INTRODUCTION

For future communication, the Federal Communications Commission (FCC) issued ultra-wideband (UWB) frequency that is unlicensed ranging from 3.1 to 10.6 GHz in 2002. It was designed originally for radar imaging, but it now permits users to have access to high-speed data transmission services [1]. Because an antenna is an important component of communication systems, researchers face a difficult challenge in designing a suitable antenna layout. As a result, due to a variety of enchanting characteristics such as small size, light weight, and fabrication flexibility, microstrip antennas have piqued the interest of researchers [2]. UWB antennas, on the other hand, have grown in popularity as a result of advantages such as high data sharing, high data transmission rate, and low power consumption [3]. However, UWB antennas suffer from multi-path fading effects, which can be reduced by using MIMO technology, which increases transmission capacity and diversity gain [4, 5]. This method allows for the use of numerous antennas to simultaneously broadcast and receive radio signals. Mutual coupling is predominant due to the close proximity between numerous antennas. Various MIMO antennas for UWB applications are demonstrated in [6–8] to reduce interference caused by close proximity of antenna elements and to increase isolation. However, within the defined UWB range, various interfering bands such as WiMAX (3.3–3.8 GHz), C-band (4–4.9 GHz), WLAN (5.1–5.8 GHz),

Received 26 November 2021, Accepted 28 December 2021, Scheduled 4 January 2022

* Corresponding author: Ramesh Babu Sadineni (srameshbabu@rvrjc.ac.in).

[1] Department of ECE, R.V.R & J.C College of Engineering, Guntur 522019, India. [2] Department of ECE, Dayananda Sagar College of Engineering, Bengaluru 560078, India.

as well as X-band satellite communication (7.7–8.4 GHz) pose significant challenges for UWB MIMO antennas [9–14]. These interfering bands have the potential to significantly reduce antenna performance. As a result, a multi-band filtering antenna is required to reject the interfering bands. A crescent ring was etched on two circular radiators in order to produce 5 GHz notch frequency [15]. A UWB antenna which operates in duple band (WiMAX/WLAN) is suggested for multiple-input-multiple-output/diversity applications consisting of a square radiator embedded with a T-shape stub and two U-shape parasitic strips adjacent to the feed line [16]. [17–19] show UWB MIMO antennas with two fold notch capabilities with mutual coupling less than −10 dB. In [20–26], various miniaturized UWB MIMO antennas with triple band notches and isolation less than −15 dB are reported. The notches were implemented using slots and EBG structures. [27–34] exhibit quad notched band behaviour with low mutual coupling. A novel miniaturized 4-slot antenna elements with a common rhombic slot for tri-notch characteristics is reported in [35]. The isolation of −25 dB along with four notches with the aid of slots and EBG is reported in [36]. A compact two port MIMO antenna which comprises two octagonal shape elements with a stub on ground and a slot on patch to reject duple band frequencies is reported in [37] for the rejection of most of the EM interference. By incorporating v-shape slots on pentagonal shape patch and a hexagonal shape EBG next to the feed, dual notches are achieved in [38]. A CPW-fed 4-port MIMO antenna which consists of TSESC patches for the elimination triple frequencies is introduced in [39]. A compact multi-band antenna with isolation using square SRRs is detailed in [40].

The literature focuses on improving UWB MIMO antenna isolation and compactness only. Steady gain along with more band notched features, on the other hand, necessitates further research. It is essential to reject a significant number of bands in order to diminish interference to a negligible level. In the literature, there were no MIMO antenna designs reported with penta-band notch behavior. As a result, in this study we report a UWB MIMO antenna with penta-band notch behavior which has excellent gain and isolation. The potential limitation of this study is bulkiness which should be taken care of in further research. The manuscript is organized as follows. Implementation of the unit element for the UWB-MIMO antenna is furnished in Section 2. Next, the implementation of UWB MIMO antenna using the unit element with reflection coefficient analysis is described in Section 3. The analysis of diversity performance metrics is described in Section 4. Section 5 concludes the article.

2. UWB UNIT ELEMENT ANTENNA CONFIGURATION

Figures 1(a) and 1(b) portray the layout of the proposed UWB unit antenna element structure. The proposed design makes use of a modified microstrip patch with a defected ground plane, engraved on

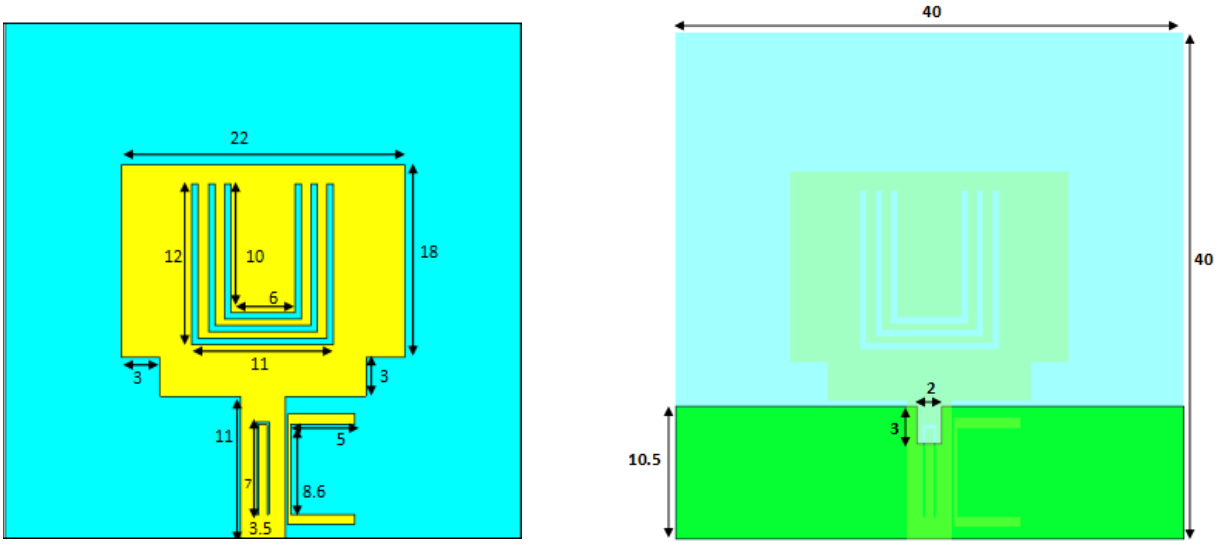

(a) (b)

Figure 1. Layout of the UWB unit element antenna (units: mm). (a) Front-view, (b) back-view.

a 1.6 mm thick Rogers RT/Duroid 5880 substrate having relative permittivity (ε_r) 2.2 with overall size of $40 \times 40\,\text{mm}^2$ or $0.4\lambda_0 \times 0.4\lambda_0$. For wider impedance bandwidth, a tiny slot was etched over the ground plane. Three U-shape slots are introduced over the surface of the antenna element and an inverse U-shape slot on the feed line in order to impede the current distribution at 3.4 GHz, 4 GHz, 4.6 GHz, and 5.7 GHz. Apart from this, a C-shaped stub is introduced adjacent to the feed line for the frequency notch at 7.8 GHz. The following formulae are used to calculate the preliminary dimensions of the proposed antenna structure [2].

The patch width (W) has been calculated by

$$W = \frac{c}{2f_r}\sqrt{\frac{2}{\varepsilon_r + 1}} \tag{1}$$

$$\varepsilon_{eff} = \frac{\varepsilon_r + 1}{2} + \frac{\varepsilon_r - 1}{2}\left(\frac{1}{\sqrt{1 + \frac{2h}{W}}}\right) \tag{2}$$

The change in length because of fringing fields is calculated by

$$\Delta L = 0.412h\frac{(\varepsilon_{eff} + 0.3)\left(\frac{W}{h} + 0.264\right)}{(\varepsilon_{eff} - 0.258)\left(\frac{W}{h} + 0.8\right)} \tag{3}$$

The patch length (L) has been calculated by

$$L = \frac{c}{2f_r\sqrt{\varepsilon_{eff}}} - 2\Delta L \tag{4}$$

The feed line width W_f and length L_f are calculated by

$$W_f = \frac{0.07 * c}{f_r\sqrt{\varepsilon_{eff}}} \tag{5}$$

$$L_f = \frac{0.3 * c}{f_r\sqrt{\varepsilon_{eff}}} \tag{6}$$

The ground plane width W_g and length L_g are calculated by Equations (7) and (8).

$$W_g = \frac{0.32 * c}{f_r\sqrt{\varepsilon_{eff}}} \tag{7}$$

$$L_g = \frac{0.28 * c}{f_r\sqrt{\varepsilon_{eff}}} \tag{8}$$

The substrate length and width are calculated by Equation (9) where $W_{sub} = L_{sub} = 40\,\text{mm}$

$$W_{sub} = L_{sub} = 6h + W \tag{9}$$

Optimization and simulation of the reported structure are done using CST MW studio 2016. Figure 2(a) depicts the fabricated antenna prototype, and Figure 2(b) depicts the simulated as well as measured S-parameter (S_{11}) in dB. The measured and simulated findings are very close to each other. The measured reflection coefficient is less than $-10\,\text{dB}$ across the entire operating band. Fabrication tolerance is responsible for the gap between simulated and measured results.

3. MIMO ANTENNA CONFIGURATION

The unit element that accomplishes the broad band operation was used to design two port and quadruple-port UWB-MIMO antennas. Figure 3(a) depicts a MIMO antenna in which the two antenna elements are arranged in a linear configuration with edge-to-edge spacing $0.2\lambda_0$. The suggested

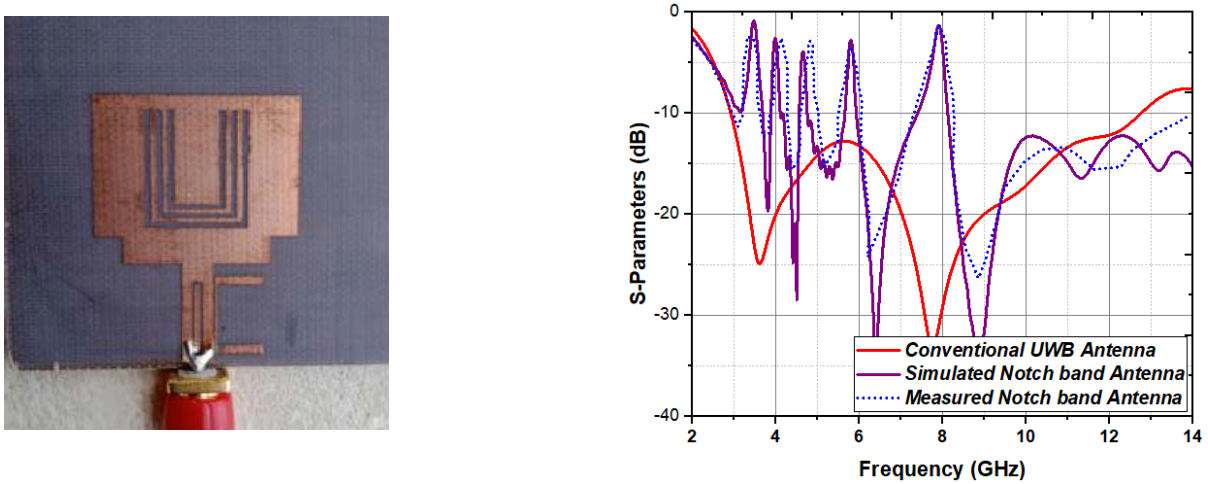

Figure 2. (a) Constructed unit-element antenna. (b) Reflection coefficient $|S_{11}|$ versus frequency.

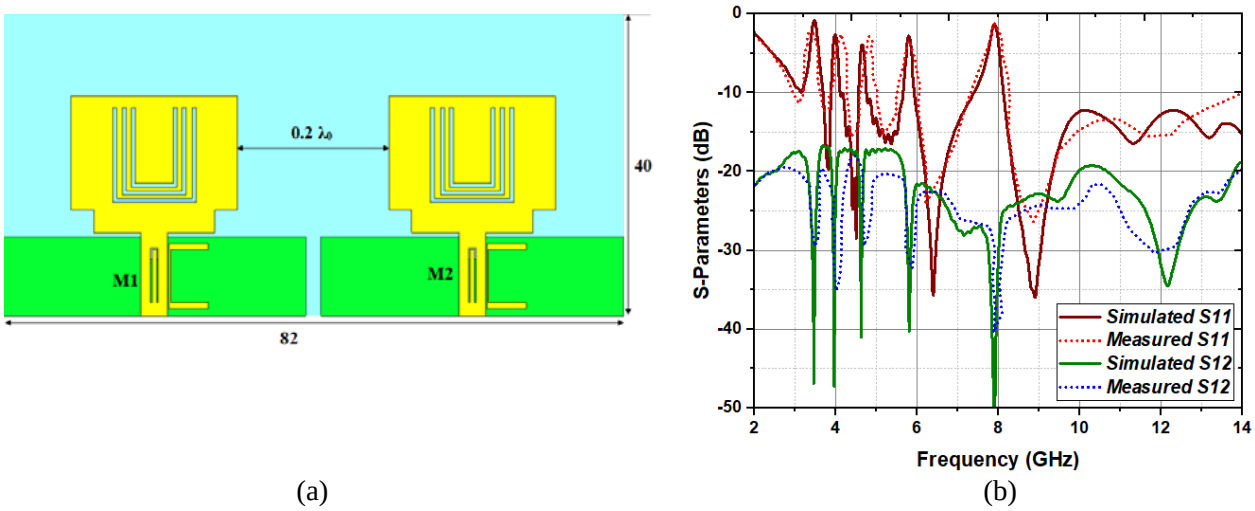

Figure 3. 2-element UWB-MIMO linear antenna. (a) Layout, (b) reflection coefficient versus frequency.

UWB MIMO antenna is imprinted over a Rogers RT/Duroid 5880 substrate having an overall size of $40 \times 82 \times 1.6\,\text{mm}^3$ or $0.4\lambda_0 \times 0.82\lambda_0 \times 0.016\lambda_0$. Figure 3(b) shows the scattering parameters that were simulated and tested. Because the antenna elements are similar, only the S-parameters S_{11} and S_{12} of port1 (M1) are examined. The collinear antenna operates between 3 GHz and 14 GHz, with notches at 3.4 GHz, 4 GHz, 4.6 GHz, 5.7 GHz, and 7.8 GHz according to the S_{11} specifications of the antenna. The two element coupling is determined by the S_{12} characteristics of the collinear antenna. In the whole working bandwidth, isolation is less than -18 dB, with particularly strong isolation at 3.4 GHz, 4 GHz, 4.6 GHz, 5.7 GHz, and 7.8 GHz.

Figure 4(a) shows the MIMO antenna in which antenna elements M1 and M2 face each other (180°). The illustrated antenna is $40 \times 80 \times 1.6\,\text{mm}^3$ or $0.4\lambda_0 \times 0.8\lambda_0 \times 0.016\lambda_0$ in size and was lithographed on a Rogers RT/Duroid 5880 substrate. S_{11} and S_{12} parameter (port1) characteristics are demonstrated in Figure 4(b). It has notches at 3.4 GHz, 4 GHz, 4.6 GHz, 5.7 GHz, and 7.8 GHz, and operates from 3 GHz to 14 GHz. There is less than -20 dB isolation between the antenna elements M1 and M2.

The elements M1 and M2 are arranged orthogonal to each other to minimize the coupling between MIMO elements even further, as shown in Figure 5(a). The antenna is $40 \times 80 \times 1.6\,\text{mm}^3$

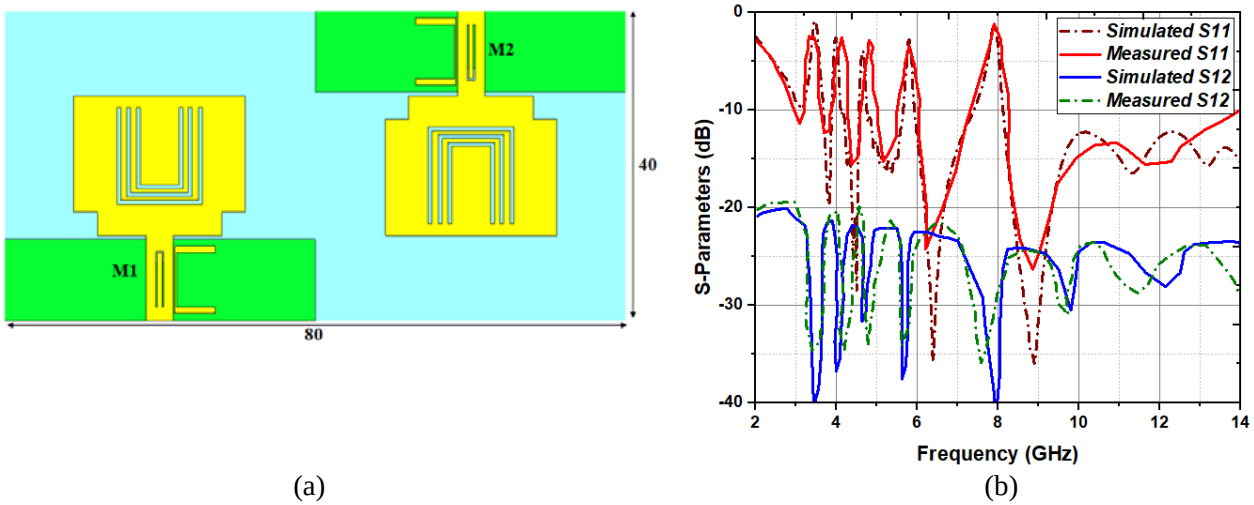

Figure 4. 2-element UWB-MIMO antenna. (a) Layout, (b) reflection coefficient versus frequency.

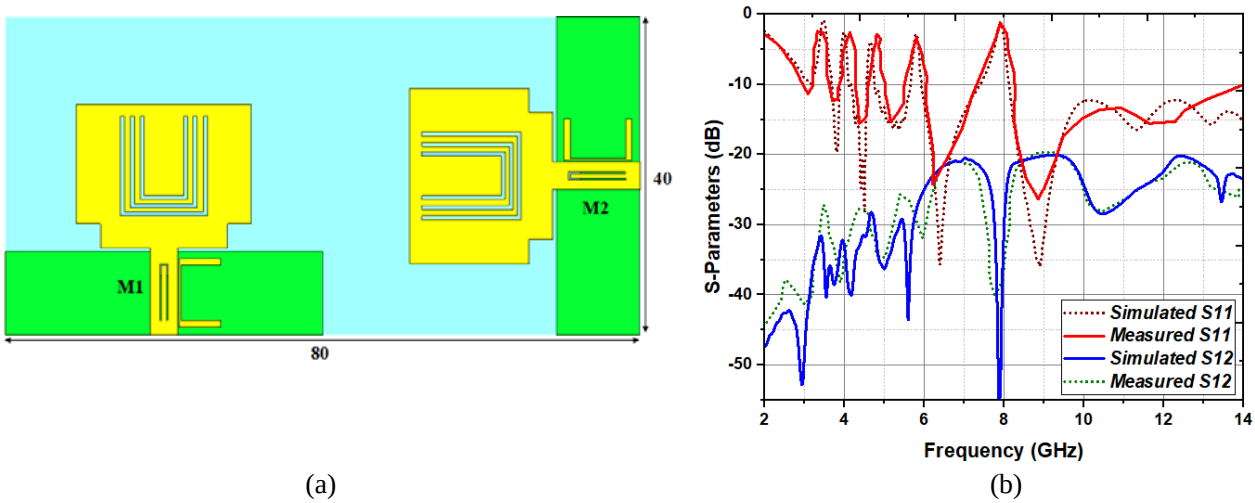

Figure 5. 2-element orthogonal UWB-MIMO antenna. (a) Layout, (b) reflection coefficient versus frequency.

or $0.4\lambda_0 \times 0.8\lambda_0 \times 0.016\lambda_0$ in size and is built on a Rogers RT/Duroid 5880 substrate. Figure 5(b) shows the MIMO antenna S-parameters for port1 (M1) excitation. It has five notches at 3.4 GHz, 4 GHz, 4.6 GHz, 5.7 GHz, and 7.8 GHz, and the coupling effect is less than -30 dB at lower frequencies and less than -20 dB for higher frequencies.

Therefore, by orienting antenna elements orthogonal to each other, mutual coupling is diminished. For gain enhancement and greater isolation, it is proposed to use a four port MIMO system with orthogonal antenna components, as shown in Figure 6(a). To lessen the coupling between elements, the MIMO model uses a split ground plane. As the MIMO antenna does not have a common ground, the antenna's reliability is lowered because its behaviour can differ between devices.

To address it, split ground planes of four MIMO antenna components are connected unitedly using 0.5 mm wide connecting strips to form a common ground which is depicted in Figure 6(b). Figure 6(c) depicts the top and bottom views of the reported antenna system. The measured as well as simulated reflection coefficients S_{11}, S_{12}, S_{13}, and S_{14} of the antenna reported, for port1 excitation are depicted in Figure 6(d). The reported antenna attained a broad impedance bandwidth ($S_{11} < -10$ dB) of 11 GHz from 3 GHz to 14 GHz with penta-band notch characteristics at 3.4 GHz, 4 GHz, 4.6 GHz, 5.7 GHz, and

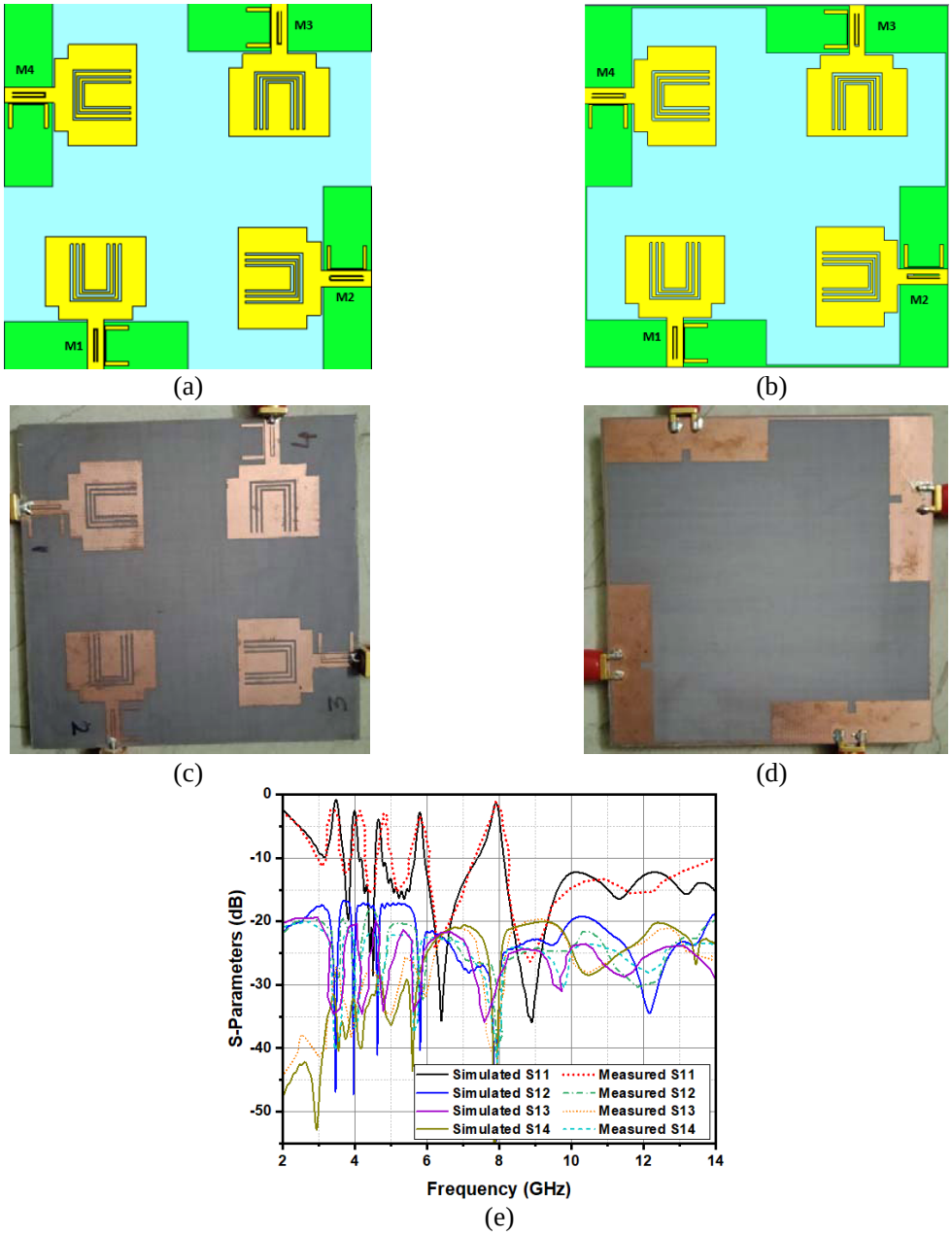

Figure 6. Suggested MIMO antenna with (a) split ground plane, (b) connected ground plane, (c) photograph of the prototype model top-view, (d) bottom-view, (e) scattering parameters of the reported 4-element UWB MIMO antenna.

7.8 GHz. Over the full operational range, the average isolation of proposed antenna is more than −20 dB. The observed and modeled scattering parameter characteristics correspond well in all circumstances, demonstrating that the reported four port orthogonal UWB-MIMO antenna is appropriate for UWB applications.

4. PARAMETRIC ANALYSIS

The critical parameters of the band-notch antenna are center frequency as well as bandwidth of the rejection band. To explore the effects of numerous parameters over the performance of the antenna, a

comprehensive parametric study has been conducted by tuning only one parameter keeping all others constant. For simplicity, only the length of the slots is varied.

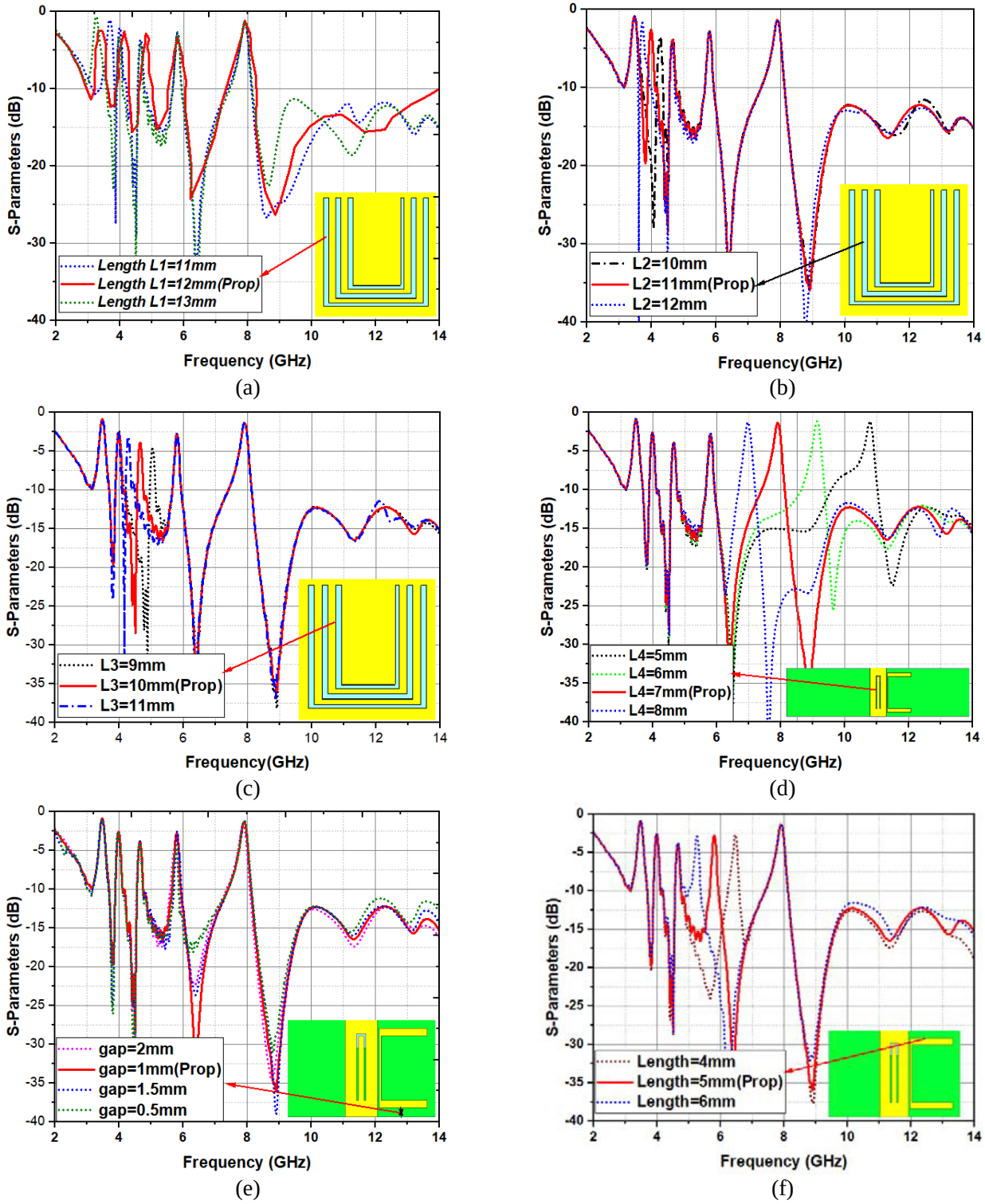

Figure 7. Simulated S_{11} plot for (a) various lengths of outer slot, (b) various lengths of middle slot, (c) various lengths of inner slot, (d) various lengths of slot on feed line, (e) variation of gap from the edge of ground plane, (f) change in lengths of C-shape stub.

Figure 7(a) depicts the effect of the length variation of the outer slot. It can be observed that when the length of the outer slot ($L1$) increases the peak of the notch shifts towards lower frequency band. In order to have notch at 3.4 GHz, the optimized parameter of the outer slot is chosen to be $L1 = 12$ mm. Furthermore, when the length of the middle slot is increased from 10 to 12 mm, the second notch peak shifts from 4.2 GHz to 3.8 GHz. For having notch frequency at 4 GHz, the optimized length of middle slot is chosen to be 11 mm which is depicted in Figure 7(b). Figure 7(c) reveals the outcome of varying the length of inner slot. It shows that as the length increases from 9 to 11 mm, the third notch band moves towards lower frequency region. With respect to having notch frequency at 4.6 GHz, the length of the inner slot is chosen to be $L3 = 10$ mm. The outcome of varying the length of the slot on feed line is demonstrated in Figure 7(d). It shows that as the length increases from 5 to 8 mm the X-band notch frequency moves towards lower frequency band. Furthermore, Figure 7(e) depicts the consequence of varying the gap between the bottom edge of c-shape stub and ground plane. It could be observed that by intensifying the gap from 0.5 to 2 mm the antenna does not show much variation apart from having more negative peak for the fourth notch band. Consequently when the horizontal section length of c-shape stub varies from 4 to 6 mm, the center frequency of the notch band shifts from 6.2 GHz to 4.6 GHz. Thus, the optimized value of the gap and horizontal section length of stub are chosen to be 1 mm and 5 mm.

5. RESULT ANALYSIS

5.1. Surface Current Density

Figure 8 depicts surface current density of the suggested MIMO antenna at indentation frequencies (3.4 GHz, 4.6 GHz, 5.7 GHz, 7.8 GHz) and the frequency at which antenna radiates (8.5 GHz), used

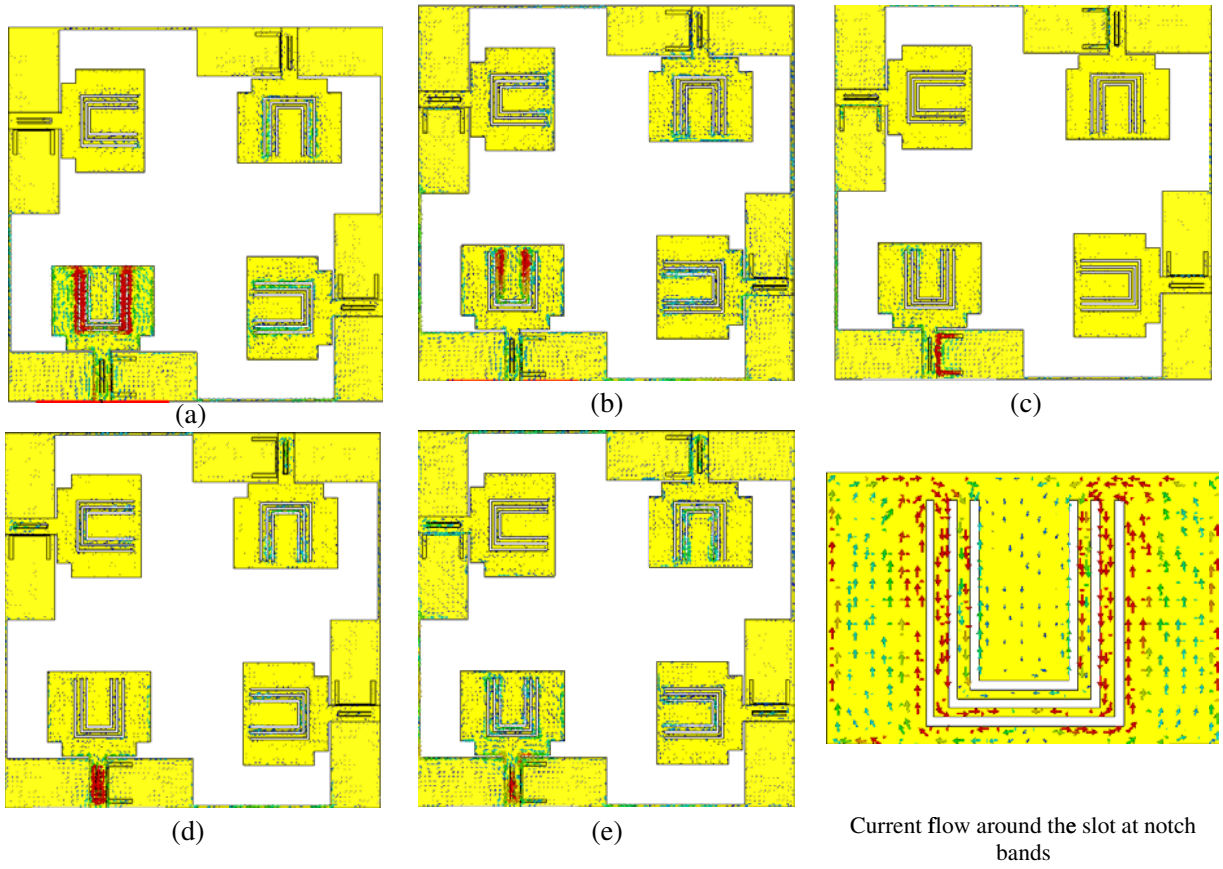

Figure 8. Surface current distribution (a) 3.4 GHz, (b) 4.6 GHz, (c) 5.7 GHz, (d) 7.8 GHz, (e) 8.5 GHz.

to better understand the phenomenon underlying the penta band-stop performance. As depicted in Figure 7, the surface current is concentrated more at the outer U-shaped slot for 3.4 GHz (WiMAX band rejection), at inner slot for 4.6 GHz (c-band rejection), at C-shaped stub for 5.7 GHz (WLAN band rejection), and at inverse U-shaped slot for 7.8 GHz (X-band downlink rejection). Furthermore, at notches the large current distributions surrounding stub/slots counteract near field radiation, resulting in high energy reverting back to the input port and hence notched behavior being realized. Because the created opposing currents cancel each other out, the resultant radiation is comparatively lower at notch frequencies as depicted in Figure 8. Furthermore, except for the band-notch, the surface current spreads equally throughout the antenna across the whole frequency passband. As a result, the suggested 4-element MIMO antenna offers better diversity properties.

5.2. Radiation Patterns

Figure 9 illustrates the simulated as well as measured co-pol and cross-pol radiation characteristics of the designed MIMO antenna at frequencies 4.4 GHz and 8.5 GHz. A difference higher than 10 dB can be observed between co-pol and cross-pol characteristics. The steady working of the designed antenna may be noticed among the co-polar and cross-polar pattern curves (in the E- and H-planes). The E-plane

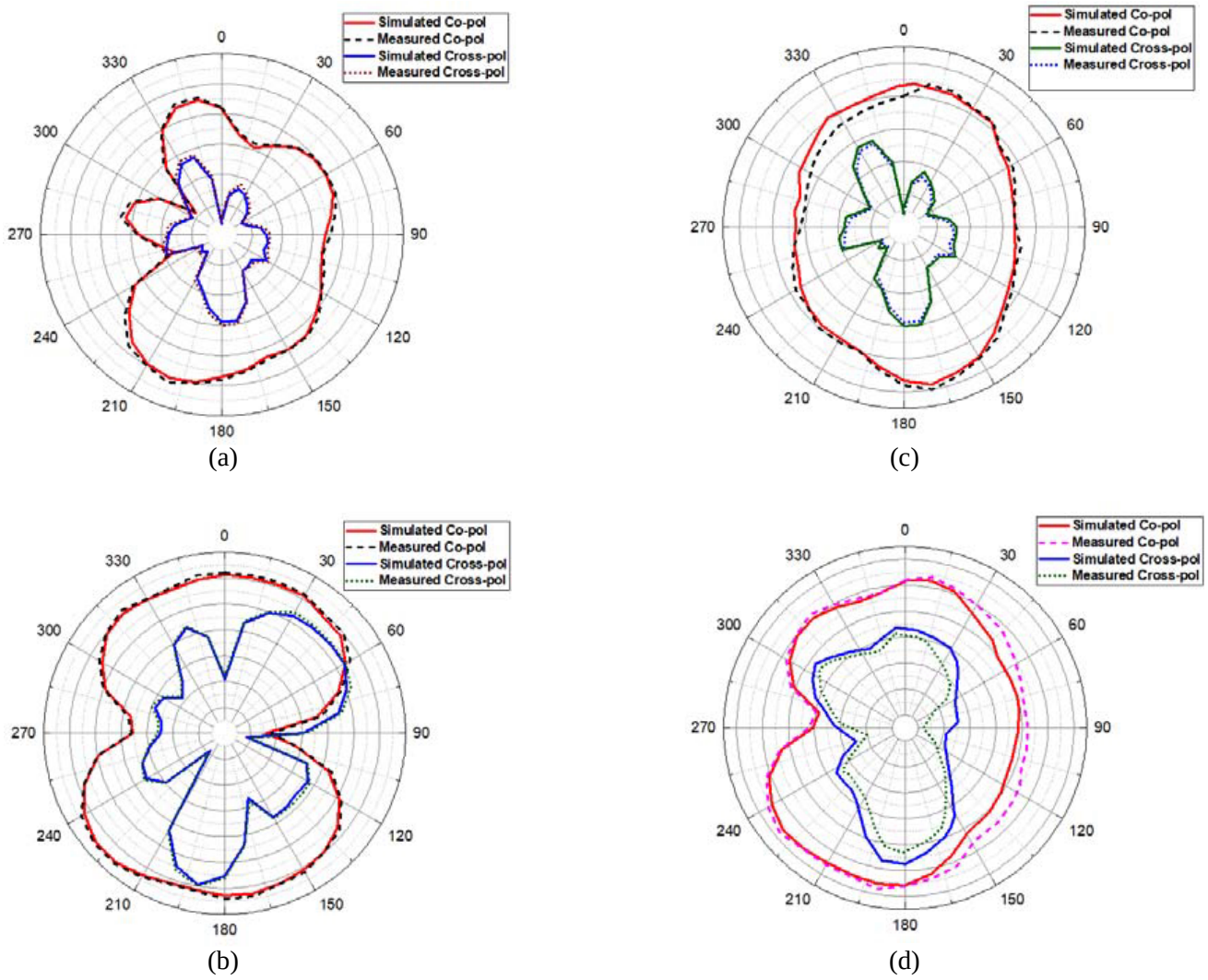

Figure 9. Radiation patterns at (a) 4.4 GHz (E-plane), (b) 4.4 GHz (H-plane), (c) 8.5 GHz (E-plane), (d) 8.5 GHz (H-plane).

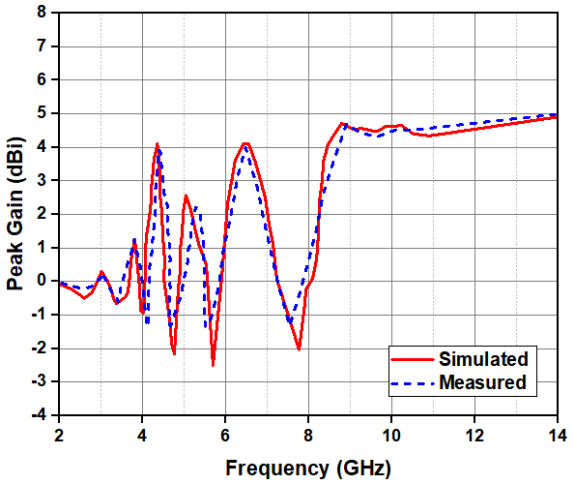

Figure 10. Simulated and measured peak gain variation over the whole impedance bandwidth.

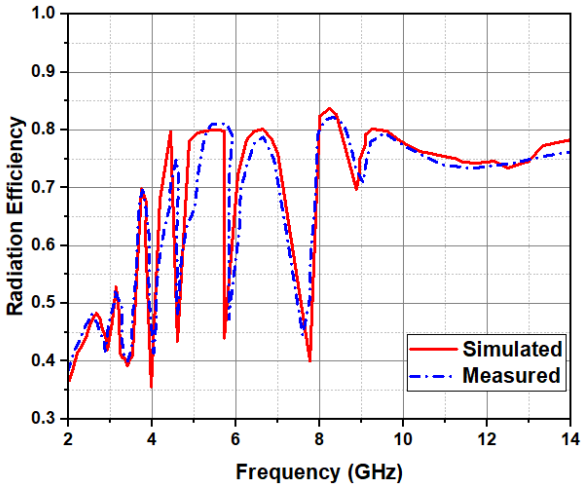

Figure 11. Simulated and measured Radiation efficiency variation over the whole impedance bandwidth.

co-polar patterns exhibited semi-omnidirectional behaviour, whereas the H-plane co-polar patterns exhibited omnidirectional activity. The consistency of simulated and experimental outcomes certifies the design's accuracy. The variations among simulated an measured co-pol and cross-pol radiation patterns are within acceptable range. Figure 10 shows gain comparison plots between simulated and measured values of the suggested UWB-MIMO antenna. At lower frequencies, gain is less and is enhanced as the frequency advances. Gain, on the other hand, diminishes dramatically at notch frequencies. In the UWB, a peak gain of 4.8 dBi is attained. As a result, the suggested 4-element MIMO antenna has good notched band performance. For port1 (M1) excitation, Figure 11 shows simulated and observed radiation efficiency values. The suggested UWB-MIMO antenna has the typical efficiency of above 83%. In contrast, it falls under 45% at notch frequencies.

5.3. MIMO Performance Metrics

5.3.1. Envelope Correlation Coefficient (ECC)

The envelope correlation coefficient (ECC), diversity gain (DG), total active reflection coefficient (TARC), and channel capacity loss (CCL) are critical parameters for validating UWB-MIMO antenna capability and performance. To portray the mutual coupling between different antenna elements ECC is used. ECC should be lower so as to achieve greater diversity among UWB-MIMO antenna elements.

$$\mathrm{ECC} = \frac{\left|\int_0^{2\pi}\int_0^{\pi}\left(XPRE_{\theta 1}E^*_{\theta 2}P_\theta + E_{\varphi 1}E^*_{\varphi 2}P_\varphi\right)d\Omega\right|^2}{\int_0^{2\pi}\int_0^{\pi}\left(XPRE_{\theta 1}E^*_{\theta 1}P_\theta + E_{\varphi 1}E^*_{\varphi 1}P_\varphi\right)d\Omega X\left(XPRE_{\theta 2}E^*_{\theta 2}P_\theta + E_{\varphi 2}E^*_{\varphi 2}P_\varphi\right)d\Omega} \tag{10}$$

ECC of a MIMO antenna can be computed using radiation patterns, as shown in Equation (10) [12, 28]. To achieve fine diversity, the ECC of any MIMO antenna ought to be under 0.5. Figure 12 shows that simulated and measured ECCs are below 0.03 across the whole UWB range, excluding rejection frequencies. At notch frequencies, the measured ECC is also lower than 0.05. Consequently, the suggested MIMO antenna does have a good diversity with less ECC values.

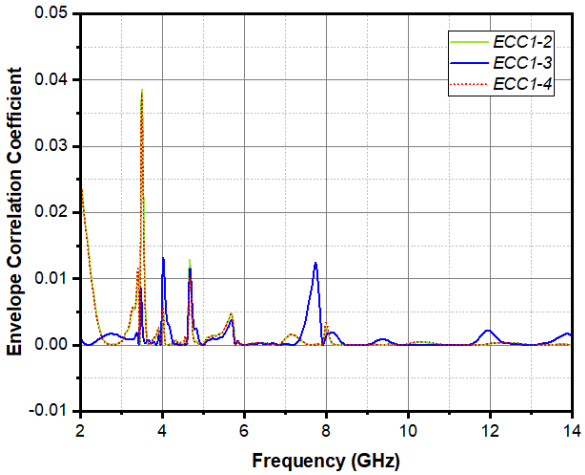

Figure 12. Envelope correlation coefficient between MIMO antenna elements.

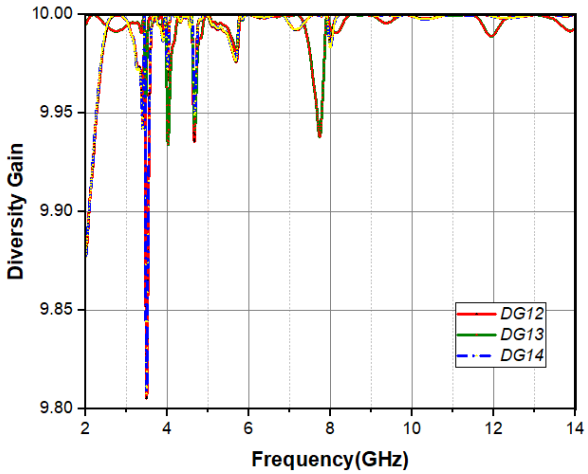

Figure 13. Diversity gain between MIMO antenna elements.

5.3.2. Diversity Gain (DG)

Diversity gain is an important performance parameter of any UWB-MIMO antenna given in Equation (11)

$$\mathrm{DG} = 10\sqrt{1 - \mathrm{ECC}^2} \tag{11}$$

Figure 13 shows DG of the suggested UWB-MIMO antenna. Diversity gain is greater than 9.9 dBi across the whole impedance spectrum excluding five notches. It exhibits that the suggested design has smaller ECC and superior DG.

5.3.3. Total Active Reflection Coefficient (TARC)

TARC is stated as the ratio of square root of the total reflected power to the total incident power and apparent return loss of the overall MIMO antenna system [28]. The optimal operating band of UWB-MIMO antenna system is determined by TARC curves. Using Equation (12) TARC values can be calculated as

$$\mathrm{TARC} = \frac{\sqrt{\sum_{I=1}^{4} |bi|^2}}{\sqrt{\sum_{I=1}^{4} |ai|^2}} \tag{12}$$

5.3.4. Channel Capacity Loss (CCL)

In general, the UWB-MIMO antenna channel capacity elevates undeviatingly with multiple antenna elements deployed. However, owing to the existence of inter dependence between the MIMO channels, it also involves certain losses. In MIMO channel systems, the correlation between elements causes capacity loss. As a result, the CCL is a critical metric for determining the MIMO systems channel capacity. The CCL value for MIMO systems should be less than 0.4 bps/Hz. Figure 14 depicts the total active reflection coefficient (TARC) characteristics as well as channel capacity loss (CCL) of the suggested four element MIMO antenna.

This shows that excluding notch frequencies, CCL and TARC values are less than 0.35 bps/Hz and −10 dB, respectively across the functional bandwidth. It exemplified that the antenna performs well enough in terms of diversity. To highlight the quintessence of the proposed research, a comparison of numerous parameters of the proposed study with already existing antennas is listed in Table 1.

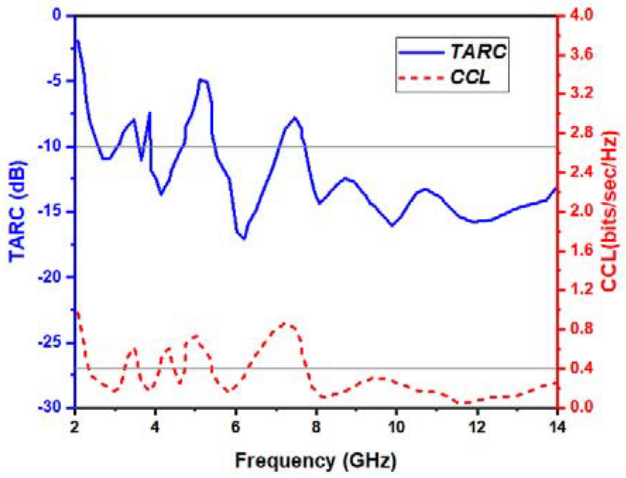

Figure 14. TARC and CCL versus frequency for the UWB-MIMO antenna.

Table 1. Performance comparison: Suggested UWB-MIMO antenna with contemporary existing antenna models.

Ref.	Area λ_0^2 (calculated at lower frequency)	Operating Band (GHz)	No. of Notch bands	Gain (dBi)	Isolation (dB)	ECC	TARC	CCL
[6]	0.095	2.9–10.6	NA	6.5	> 15	< 0.2	NA	< 0.4
[12]	0.096	3.1–11	1	5	> 20	< 0.02	< -10	< 0.35
[21]	0.134	3.1–10.6	1	5.2	> 20	< 0.02	NA	< 0.4
[22]	0.196	2.5–11	3	6	> 15	< 0.02	NA	NA
[8]	0.17	3.1–11	NA	4	> 20	< 0.01	NA	< 0.4
[9]	0.122	3.0–12.0	1	NA	> 20	< 0.3	NA	NA
[10]	0.09	2.0–10.6	1	4	> 17	< 0.01	NA	< 0.4
[30]	0.16	2.7–12	1	5.5	> 17	< 0.03	NA	NA
[32]	0.16	2.7–12	1	6	> 17	NA	NA	NA
Proposed	**0.64**	**3–14**	**5**	**4.8**	$\mathbf{> 20}$	$\mathbf{< 0.02}$	$\mathbf{< -13}$	$\mathbf{< 0.3}$

6. CONCLUSION

A penta-band notched ultra-wideband MIMO antenna with diverse wireless applications has been efficaciously modeled and simulated. The suggested four port UWB MIMO antenna exhibits a large functional bandwidth covering from 3 to 14 GHz and is suitable to oppose five intrusive frequencies (3.4 GHz, 4 GHz, 4.6 GHz, 5.7 GHz, and 7.8 GHz respectively). With these notches WiMAX, C-band, WLAN, and X-band interference can be filtered out. The diversity performance metrics are evaluated by amending single port antenna into a four port UWB-MIMO antenna. A few of the antenna performance attributes investigated include reflection coefficient, current distribution on antenna surface, far-field radiation patterns, ECC, DG, TARC, and CCL. In the operational band, radiation efficiency higher than 83% excluding notches, with a peak gain of 4.8 dBi, is achieved. The design features excellent isolation less than -20 dB, ECC less than 0.03, diversity gain of approximately 10, TARC less than -10 dB, and CCL less than 0.35 bps/Hz. As a result, the suggested four-element UWB-MIMO antenna is affirmed as a feasible candidate for a variety of wireless applications.

REFERENCES

1. Federal Communications Commission, "Revision of Part 15 of the Commission's rules regarding ultra-wideband transmission system from 3.1 to 10.6 GHz," ET-Docket, 98–153, Federal Communications Commission, Washington, DC, 2002.
2. Balanis, C. A., *Antenna Theory Analysis and Design*, 3rd Edition, Chapter 14, 811–872, John Wiley & Sons, Inc., 2005.
3. Abbosh, M., "A design of a CPW-fed band-notched UWB antenna using a feeder embedded slot-line resonator," *International Journal of Antennas and Propagation*, Vol. 2008, 1–5, 2008.
4. Lee, Y., D. Ga, and J. Choi, "Design of a MIMO antenna with improved isolation using MNG metamaterial," *International Journal of Antennas and Propagation*, Vol. 2012, 1–7, 2012.
5. Babu, K. J., R. W. Aldhaheri, M. Y. Talha, and I. S. Alruhaili, "Design of a compact two element MIMO antenna system with improved isolation," *Progress In Electromagnetics Research Letters*, Vol. 48, 27–32, 2014.
6. Liu, L., S. W. Cheung, and T. I. Yuk, "Compact MIMO antenna for portable devices in UWB applications," *IEEE Transactions on Antennas and Propagation*, Vol. 61, No. 8, 4257–4264, 2013.
7. Khan, M. K., Q. Feng, and Z. Zheng, "Experimental investigation and design of UWB MIMO antenna with enhanced isolation," *Progress In Electromagnetics Research C*, Vol. 107, 287–297, 2021.
8. Ali, W. A. E. and A. A. Ibrahim, "A compact double-sided MIMO antenna with an improved isolation for UWB applications," *AEU-International Journal of Electronics and Communications*, Vol. 82, 7–13, 2017.
9. Zhu, J., S. Li, B. Feng, L. Deng, and S. Yin, "Compact dual-polarized UWB quasi-self-complementary MIMO/diversity antenna with band-rejection capability," *IEEE Antennas and Wireless Propagation Letters*, Vol. 15, 905–908, 2016.
10. Tripathi, S., A. Mohan, and S. Yadav, "A compact Koch fractal UWB MIMO antenna with WLAN band-rejection," *IEEE Antennas and Wireless Propagation Letters*, Vol. 14, 1565–1568, 2015.
11. Iqbal, A., O. A. Saraereh, A. W. Ahmad, and S. Bashir, "Mutual coupling reduction using F-shaped stubs in UWB-MIMO antenna," *IEEE Access*, Vol. 6, 2755–2799, 2018.
12. Biswal, S. P. and S. Das, "A low-profile dual port UWB-MIMO/diversity antenna with band rejection ability," *International Journal of RF and Microwave Computer Aided Engineering*, Vol. 28, No. 1, 2017.
13. Nouri, A. and G. R. Dadaszadeh, "A compact UWB band-notched printed monopole antenna with defected ground structure," *IEEE Antennas and Wireless Propagation Letters*, Vol. 10, 1178–1182, 2011.
14. Chandel, R. and A. K. Gautam, "Compact MIMO/diversity slot antenna for UWB applications with band-notched characteristic," *Electronics Letters*, Vol. 52, No. 5, 336–338, 2016.
15. Kumar, A., A. Q. Ansari, B. Kanaujia, J. Kishor, and N. Tewari, "Design of triple-band MIMO antenna with one band-notched characteristic," *Progress In Electromagnetic Research C*, Vol. 86, 41–53, 2018.
16. Jiang, W. and W. Che, "A novel UWB antenna with dual notched bands for WiMAX and WLAN applications," *IEEE Antennas and Wireless Propagation Letters*, Vol. 11, 293–296, 2012.
17. Li, J. F., Q. X. Chu, Z. H. Li, and X. X. Xia, "Compact dual band-notched UWB MIMO antenna with high isolation," *IEEE Transactions on Antennas and Propagation*, Vol. 61, No. 9, 4759–4766, 2013.
18. Li, Z., C. Yin, and X. Zhu, "Compact UWB MIMO Vivaldi antenna with dual band-notched characteristics," *IEEE Access*, Vol. 7, 38696–38701, 2019.
19. Zhou, D., S. Gao, F. Zhu, R. A. Abd-Alhameed, and J.-D. Xu, "A simple and compact planar ultra wideband antenna with single OR dual band-notched characteristics," *Progress In Electromagnetics Research*, Vol. 123, 47–65, 2012.

20. Tang, Z., X. Wu, J. Zhan, S. Hu, Z. Xi, and Y. Liu, "Compact UWB-MIMO antenna with high isolation and triple band-notched characteristics," *IEEE Access*, Vol. 7, 19856–19865, 2019.
21. Yadav, D., M. P. Abegaonkar, S. K. Koul, V. N. Tiwari, and D. Bhatnagar, "Two element band-notched UWB MIMO antenna with high and uniform isolation," *Progress In Electromagnetics Research M*, Vol. 63, 119–129, 2018.
22. Jaglan, N., S. D. Gupta, E. Thakur, D. Kumar, B. K. Kanaujia, and S. Srivastava, "Triple band notched mushroom and uniplanar EBG structures based UWB MIMO/diversity antenna with enhanced wide band isolation," *AEU-International Journal of Electronics and Communications*, Vol. 90, 36–44, 2018.
23. Zarrabi, F. B., Z. Mansouri, N. P. Gandji, and H. Kuhestani, "Triple-notch UWB monopole antenna with fractal Koch and T-shaped stub," *International Journal of Electronics and Communications*, Vol. 70, 64–69, 2016.
24. Srivastava, G., S. Dwari, and B. K. Kanaujia, "A compact triple band notch circular ring antenna for UWB applications," *Microwave and Optical Technology Letters*, Vol. 57, No. 3, 668–672, 2015.
25. Khandelwal, M. K., B. K. Kanaujia, S. Dwari, S. Kumar, and A. K. Gautam, "Triple band circularly polarized compact microstrip antenna with defected ground structure for wireless applications," *International Journal of Microwave and Wireless Technologies*, Vol. 8, 1–11, 2015.
26. Doddipalli, S. and A. Kothari, "Compact UWB antenna with integrated triple notch bands for WBAN applications," *IEEE Access*, Vol. 7, 183–190, 2019.
27. Naktong, W. and A. Ruengwaree, "Four port rectangular monopole antenna for UWB-MIMO applications," *Progress In Electromagnetics Research B*, Vol. 87, 19–38, 2020.
28. Rahman, M., D.-S. Ko, and D. J. Park, "A compact multiple notched ultra-wide band antenna with an analysis of the CSRR-TO-CSRR coupling for portable UWB applications," *Sensors*, Vol. 17, 2174, 2017.
29. Chandel, R., A. K. Gautam, and K. Rambabu, "Design and packaging of an eye-shaped multiple-input-multiple-output antenna with high isolation for wireless UWB applications," *IEEE Transactions on Components, Packaging and Manufacturing Technology*, Vol. 8, No. 4, 635–642, 2018.
30. Khan, S. M., A. Iftikhar, S. M. Asif, A. D. Capobianco, and B. D. Braaten, "A compact four elements UWB MIMO antenna with on-demand WLAN rejection," *Microwave and Optical Technology Letters*, Vol. 58, No. 2, 270–276, 2016.
31. Wu, W., B. Yuan, and A. Wu, "A quad-element UWB-MIMO antenna with band-notch and reduced mutual coupling based on EBG structures," *International Journal of Antennas and Propagation*, Vol. 2018, 1–10, 2018.
32. Khan, M. S., B. D. Braaten, A. Iftikhar, A. D. Capobianco, B. Ijaz, and S. Asif, "Compact 4×4 UWB-MIMO antenna with WLAN band rejected operation," *Electronics Letters*, Vol. 51, 1048–1050, 2015.
33. Wu, L., Y. Xia, X. Cao, and Z. Xu, "A miniaturized UWB-MIMO antenna with quadruple band-notched characteristics," *International Journal of Microwave and Wireless Technologies*, Vol. 10, 948–955, 2018
34. Wu, L., Y. Xia, and X. Cao, "Design of compact quad-band notched UWB-MIMO antenna," *Wireless Personal Communications*, Vol. 98, 225–236, 2018.
35. Chen, Z., W. Zhou, and Z. Hong, "A miniaturized MIMO antenna with triple band-notched characteristics for UWB applications," *IEEE Access*, Vol. 9, 63646–63655, 2021.
36. Modak, S. and T. Khan, "A slotted UWB-MIMO antenna with quadruple band-notch characteristics using mushroom EBG structure," *International Journal of Electronics and Communications*, Vol. 134, 1–6, 2021.
37. Kumar, A., Q. A. Ansari, K. B. Kanaujia, J. Kishor, and S. Kumar, "An ultra compact two-port UWB MIMO antenna with dual band notched characteristics," *AEU-International Journal of Electronics and Communications*, Vol. 114, 1–12, 2020.

38. Kadam, A. A. and A. A. Deshmukh, "Pentagonal shaped UWB antenna loaded with slot and EBG structure for dual band notched response," *Progress In Electromagnetics Research M*, Vol. 95, 165–176, 2020.
39. Kumar, P., S. Urooj, and F. Alrowais, "Design of quad-port MIMO/diversity antenna with triple-band elimination characteristics for super-wideband applications," *Sensors*, Vol. 20, 1–12, 2020.
40. Kumar, A., A. Q. Ansari, B. K. Kanaujia, and J. Kishor, "High isolation compact four-port MIMO antenna loaded with CSRR for multiband applications," *Frequenz*, Vol. 72, Nos. 9–10, 415–427, 2018.